



HAL
open science

Impact of the vibration measurement points geometric coordinates uncertainties on two-dimensional k-space identification: Application to a sandwich plate with honeycomb core

Ramzi Lajili, Khaoula Chikhaoui, Zakaria Zergoune, Mohamed Lamjed Bouazizi, Mohamed Ichchou

► To cite this version:

Ramzi Lajili, Khaoula Chikhaoui, Zakaria Zergoune, Mohamed Lamjed Bouazizi, Mohamed Ichchou. Impact of the vibration measurement points geometric coordinates uncertainties on two-dimensional k-space identification: Application to a sandwich plate with honeycomb core. *Mechanical Systems and Signal Processing*, 2022, 167, 10.1016/j.ymssp.2021.108509 . hal-04083020

HAL Id: hal-04083020

<https://hal.science/hal-04083020>

Submitted on 22 Jul 2024

HAL is a multi-disciplinary open access archive for the deposit and dissemination of scientific research documents, whether they are published or not. The documents may come from teaching and research institutions in France or abroad, or from public or private research centers.

L'archive ouverte pluridisciplinaire **HAL**, est destinée au dépôt et à la diffusion de documents scientifiques de niveau recherche, publiés ou non, émanant des établissements d'enseignement et de recherche français ou étrangers, des laboratoires publics ou privés.



Distributed under a Creative Commons Attribution - NonCommercial 4.0 International License

Impact of the vibration measurement points geometric coordinates uncertainties on two-dimensional k-space identification: Application to a sandwich plate with honeycomb core

R. Lajili¹⁻²⁻³, K. Chikhaoui⁴, Z. Zergoune¹, M.-L. Bouazizi⁵, M.-N. Ichchou¹

¹ Laboratory of Tribology and Dynamics of Systems (LTDS), Ecole Centrale de Lyon - 36 Avenue Guy de Collongues, 69130 Ecully, France.

² National School of Engineers of Tunis (ENIT), University of Tunis el Manar - BP 37 Le Belvedere, 1002 Tunis, Tunisia.

³ Preparatory Engineering Institute of Nabeul (IPEIN), Laboratory of Physics, Mathematics, Quantum Modeling and Mechanical Design, 8000 M^rrezgua, Nabeul, Tunisia.

⁴ Dupuy De Lôme Research Institute (IRDL), Centre de Recherche C. HUYGENS, Rue de Saint-Maudé - BP 92116 F-56321 Lorient Cedex, France.

⁵ Department of Mechanical Engineering, College of Engineering, Prince Sattam bin Abdulaziz University (PSAU), Alkharj 16273, Saudi Arabia.

ramzi.lajili.univ@gmail.com, chikhaoui2013@gmail.com, zergoune.uni@gmail.com, mohamedlamjed@gmail.com, mohamed.ichchou@ec-lyon.fr

Abstract

The purpose of the present paper is to investigate the wave propagation features in a sandwich plate with honeycomb core over a large frequency domain. Robust experiment-based identification processes are proposed to estimate propagation direction-dependent and frequency-dependent wavenumber-space (k-space) characteristics in presence of parametric uncertainties. These processes combine structural identification and uncertainty propagation methods. A special emphasis is put on wave correlation methods compared to two-dimensional Discrete Fourier Transform. The Variant of the Inhomogeneous Wave Correlation method is extended here to two-dimensional identification problems. The vibration field is experimentally measured at points which geometric coordinates are supposed to vary randomly. Statistical investigations are then carried out to quantify the impact of the measurement points geometric coordinates' variability on the identified parameters and evaluate the robustness of the proposed identification processes against uncertainties. Valuable insights into k-space profiles, damping loss factor and equivalent mechanical parameters, regarding the structural orthotropic behavior, are highlighted. The obtained results show the large variability of the identified parameters and reveal a significant identification sensitivity to the measurement points geometric coordinates' uncertainties. The use of the generalized Polynomial Chaos method allows robust identification with an interesting computing time reduction regarding the Latin Hypercube Sampling.

Keywords: Wide-band identification, Wavenumber-space, Honeycomb sandwich plate, Uncertainties, Robustness

1. Introduction

Composite materials form an ever-growing emphasis in engineering applications since they provide interesting characteristics such as high stiffness and lightweight. The use of composite materials allows designing lightweight structures and enables more flexibility in structural engineering. Special attention is paid to sandwich-structured composites with honeycomb cores. Such materials exhibit often an orthotropic behavior which is determined by specific properties. The characterization of such

materials is rarely obtainable from tables and does not match theoretical designs. It could be carried out experimentally using appropriate measurement techniques. Modal-based techniques are widely used and permit to extract structural elastic parameters from the measurement of resonance frequencies and mode shapes. However, they suffer mainly from a frequency constraint and require specific boundary conditions. Indeed, modal parameters are difficult to measure in the mid-high frequency domain which is characterized by strong modal overlap. Composite materials properties, in particular, could strongly vary with frequency which requires techniques with a broadband efficiency. The wave-based approach overcomes the modal-based approach limitations in the mid-high frequency domain. In a wave propagation framework, the wave-based approach permits to estimate the material properties by extracting the wave propagation features in a structure from measured data. In recent years, special attention has been paid by the scientific community to this typical inverse problem. The most identification methods used frequently in the literature are the Prony series [1], the Ferguson method [2], the Mc Daniel method [3], the Inhomogeneous Wave Correlation (IWC) [4, 5] and the Fourier Transforms (FTs). The IWC method is well suited to composite structures in particular and insensitive to boundary conditions. It consists in correlating a local vibration field with an inhomogeneous damped wave to identify the direction-dependent and frequency-dependent wavenumber and wave attenuation. The IWC is an energetic method which makes a correlation between the energy carried on by the inhomogeneous wave and the total energy of the vibrating structure. The IWC method has been recently applied by Marchetti et al. [6] in a comparative study to validate a methodology based on an analytical multilayer model of Guyader and Lesueur in the context of sandwich and laminated multilayered plates characterization in terms of wavenumber, stiffness and damping. An alternative fitting approach was proposed by Roozen et al. [7] to estimate the frequency dependent material properties of single point-excited thin isotropic plates. It consists in constructing Green's functions on the basis of Hankel's functions, using an analytical image source method [8]. The authors highlighted that the planar wave-based approximations, such that used in the IWC, are only valid in the far field since the vibration field deviates from a plane wave field near the excitation point, which requires to choose measurement points not too close to the excitation point. Recently, Marchetti et al. [9] have extended the Hankel's fitting approach for the characterization of elliptical orthotropic plates, using the equivalent thin plate theory. The validation of the approach has been performed compared to the estimations of the IWC method and an analytical model. The authors have highlighted the sensitivity of the IWC estimates to measurement noise. Moreover, an identification method based on an algorithm of the Estimation of Signal Parameters via Rotational Invariance Techniques (ESPRIT) was proposed by Margerit et al. to extract complex wavevector for 1D [10] and 2D [11] structures in wide frequency range. Besides, Tufano et al. [12] recently demonstrated the efficiency of an IWC-based inverse approach to characterize the vibration behavior of structures with different complexity levels. Its feasibility has been investigated on a plane steel panel, a curved thick composite sandwich shell and a stiffened aluminum aircraft sidewall panel, subjected to either a diffuse acoustic field or a point mechanical excitation. In this paper, a special emphasis is put on the IWC-Variant (IWC-V) which is proposed by Lajili et al. [13] to improve the inaccurate IWC estimates at low frequencies [14, 15]. The IWC-V has been applied to a honeycomb sandwich beam [13] and is extended here to two-dimensional (2D) identification problems. The IWC-V consists in correlating the vibration field with a summation of inhomogeneous waves and accounts for both forward and backward propagating waves. The IWC-V permits to identify the direction-dependent and frequency-dependent wavenumber and wave attenuation over a large frequency domain. It requires neither specific boundary conditions, nor specific geometry. Bending stiffnesses, orthotropic properties (i.e. orthotropy angle) and equivalent mechanical parameters (Young's moduli, shear modulus and Poisson's ratios) could then be extracted from the identified k-space characteristics using theoretical dispersion relations and equivalent models. In the literature, some works focus on the improvement of

the method. For instance, Cherif et al. [16] proposed an inverse wave method which applies the IWC method to estimate the damping loss factor using as input an a-priori accurately identified wavenumber by the same method. Experimental investigations of the accuracy of the inverse wave method are performed on isotropic and orthotropic honeycomb sandwich panels. An extended form of the IWC method (EIWC) was proposed by Van Belle et al. [17]. The authors include the experimental excitation location in the inhomogeneous wave expression. Roozen et al. [18] proposed to use only half of the measurement data along a line, either to the left or to the right of the excitation position, employing a Prony and IWC approach.

One of the most frequently used identification methods is that proposed by Mc Daniel et al. [3]. It consists in comparing the really measured vibration field to a created wave field. This lies in an optimization algorithm which adjusts the wavenumber and the wave attenuation at each frequency and propagation direction. The 2D Discrete Fourier Transform (2D-DFT) allows transforming the amplitude-time data to amplitude-wavenumber data at discrete frequencies. It was used by Alleyne and Cawley [19] and Bolton et al. [20] in the context of multimodal analysis to measure the amplitudes and velocities of propagating Lamb waves. The 2D-DFT was also used to approximate dispersion curves of 2D structures from measured vibratory field by Ichchou et al. [21, 22], Huang [23], Ruzek et al. [24], Zhou et al. [25, 26], Roozen et al. [27], etc. Van Damme and Zemp [28] compared the 2D-DFT and the IWC method to estimate the dispersion of bending waves, the elastic properties, and the spatial damping in beams. The 2D-DFT implementation is simple using standard Fast Fourier Transform (FFT) algorithms, but the method is very demanding in terms of computational time since a complete vibration field must be calculated and a high resolution is required for the FFT.

On the other hand, addressing such issue in deterministic framework remains a constraining hypothesis in vibration mechanics. To achieve more realistic identifications, it is inevitable to consider uncertainties and evaluate their impact on k-space characteristics. In an experiment-based identification context, uncertainties which affect the vibration field measurements are frequently encountered. For instance, the measured vibratory field may not match the associated measuring points' coordinates. The geometric variability of these coordinates is not the only influencing factor which could affect the identification process. In the context of inverse problem, since the vibratory field is the main input parameter, the most influencing parameters should be linked to its measurements. Many other parameters should be also considered for ample uncertainty analysis, which is the focus of future works. Parametric and sensitivity analyses could also be addressed to show the impact of the variability of several parameters on identifications. Only uncertainty on the geometric measurement points' coordinates is considered in this paper. Such type of uncertainty has also been considered by authors in a previous work [13] which focused on robust numerical-based and experiment-based identifications of isotropic and honeycomb sandwich beam. Here, the geometric variability of measurement points' coordinates is modeled by parametric uncertainty which is quantified probabilistically using random variables and then propagated through the identification model using uncertainty propagation methods. The sample-based uncertainty propagation methods are frequently used in literature. These methods give accurate results but are very time-consuming. The most commonly used methods are the Monte Carlo Simulations (MCS) [29, 30] and the Latin Hypercube Sampling (LHS) [31, 32]. The LHS method permits to reduce the computational time required by the MCS without a significant loss of accuracy. In practice, the number of samples is reduced by partitioning the variability space into regions of equal probability and then selecting one sampling point in each region. Alternatively, non-sample-based methods require lower computational cost. The generalized Polynomial Chaos (gPC) method has recently shown a growing emphasis [33,

34]. Its expansion combines multivariate polynomials and deterministic coefficients which could be computed using a non-intrusive regression technique [35, 36, 37].

The originality of the present paper lies in proposing robust experiment-based identification processes to identify the k-space characteristics and the equivalent mechanical parameters of a sandwich plate with honeycomb core over a large frequency domain in presence of uncertainties on the measurement points' coordinates. Some robust experiment-based identification processes are proposed here and are compared to each other. They consist in combining identification and uncertainty propagation methods. The most robust one is that combining the IWC-V with the regression-based gPC method. Its efficiency is evaluated in terms of accuracy and computing time.

2. Theoretical backgrounds

2.1. Spatial Discrete Fourier Transform

Standard Discrete Fourier Transform (DFT) allows exploring the spectral content of time signals. A spatial 2D-DFT could be used to estimate the k-space content of spatial two-dimensional fields. Then, a spatial sampling at points on a uniform discrete 2D grid $L_x \times L_y$ is made: $x_i = i\Delta x, x_j = j\Delta y$, with $0 \leq i \leq N_x - 1, 0 \leq j \leq N_y - 1$ and $N_x \times N_y$ is the number of equally distributed spatial sampling points. The displacement field u is transformed to a complex function:

$$\hat{u}(k_{xp}, k_{yq}) = \frac{1}{N_1 N_2} \sum_{i=0}^{N_1-1} \sum_{j=0}^{N_2-1} u(x_i, y_j) e^{-i(k_{xp}x_i + k_{yq}y_j)} \quad (1)$$

which could be expressed as:

$$\hat{u}(k_{xp}, k_{yq}) = \Re\{\hat{u}(k_{xp}, k_{yq})\} + i \Im\{\hat{u}(k_{xp}, k_{yq})\} \quad (2)$$

where $\Im\{\cdot\}$ and $\Re\{\cdot\}$ correspond respectively to the imaginary and real parts. $k_{xp} = p\Delta k_x$ and $k_{yq} = q\Delta k_y$ are the complex wavenumbers' exponentials, with $0 \leq p \leq N_x - 1, 0 \leq q \leq N_y - 1, k_x = K_x(1 + i\gamma_x), k_y = K_y(1 + i\gamma_y)$ and:

$$\Delta k_x = \frac{2\pi}{N_x \Delta x}; \Delta k_y = \frac{2\pi}{N_y \Delta y} \quad (3)$$

The real wavenumber k , the wave attenuation γ and the propagation direction θ are then calculated by:

$$k = \sqrt{\Re(k_x)^2 + \Re(k_y)^2} = \sqrt{K_x^2 + K_y^2} \quad (4)$$

$$\gamma = \sqrt{\left(\frac{\Im(k_x)}{\Re(k_x)}\right)^2 + \left(\frac{\Im(k_y)}{\Re(k_y)}\right)^2} = \sqrt{\gamma_x^2 + \gamma_y^2} \quad (5)$$

$$\theta = \tan^{-1}\left(\frac{\Re(k_y)}{\Re(k_x)}\right) = \tan^{-1}\left(\frac{K_y}{K_x}\right) \quad (6)$$

The 2D-DFT is $\frac{2\pi}{\Delta x}$ and $\frac{2\pi}{\Delta y}$ periodic and bijective, which allows Inverse DFT (IDFT).

2.2. Mc Daniel method

The Mc Daniel method [3] allows estimating complex wavenumbers and amplitudes of waves propagated through damped structures. It consists in iteratively adjusting the wavenumber k and the

wave attenuation γ to accurately approximate the wave field. The method is based on dispersion relations containing information about viscoelastic properties which are difficult to measure experimentally. The loss factor is considered as one of the most important properties.

Given zero initial conditions and forcing only at the boundaries, the displacement field is expressed as a sum of inhomogeneous waves:

$$u(x, y, \omega) = e^{ik(x \cos \theta + y \sin \theta)(1+i\gamma)} c_1(\omega) + e^{-ik(x \cos \theta + y \sin \theta)(1+i\gamma)} c_2(\omega) + e^{k(x \cos \theta + y \sin \theta)(1+i\gamma)} c_3(\omega) + e^{-k(x \cos \theta + y \sin \theta)(1+i\gamma)} c_4(\omega) \quad (7)$$

Given the variable transformation $X = x \cos \theta + y \sin \theta$, Eq. (7) becomes:

$$u(X, \omega) = e^{ikX(1+i\gamma)} c_1(\omega) + e^{-ikX(1+i\gamma)} c_2(\omega) + e^{kX(1+i\gamma)} c_3(\omega) + e^{-kX(1+i\gamma)} c_4(\omega) \quad (8)$$

The first two terms correspond to flexural waves and the latter to evanescent waves. Damping causes the flexural waves to decay and the evanescent waves to oscillate.

When the spatial field is measured at n discrete locations $\{X_1, X_2, \dots, X_n\}$, Eq. (8) takes the form of a system of n nonlinear complex algebraic equations at each frequency ω :

$$\begin{bmatrix} u(X_1, \omega) \\ u(X_2, \omega) \\ \vdots \\ u(X_n, \omega) \end{bmatrix} = \begin{bmatrix} e^{ikX_1(1+i\gamma)} & e^{-ikX_1(1+i\gamma)} & e^{kX_1(1+i\gamma)} & e^{-kX_1(1+i\gamma)} \\ e^{ikX_2(1+i\gamma)} & e^{-ikX_2(1+i\gamma)} & e^{kX_2(1+i\gamma)} & e^{-kX_2(1+i\gamma)} \\ \vdots & \vdots & \vdots & \vdots \\ e^{ikX_n(1+i\gamma)} & e^{-ikX_n(1+i\gamma)} & e^{kX_n(1+i\gamma)} & e^{-kX_n(1+i\gamma)} \end{bmatrix} \begin{bmatrix} c_1(\omega) \\ c_2(\omega) \\ c_3(\omega) \\ c_4(\omega) \end{bmatrix} \quad (9)$$

The wave amplitudes $\{c_1, c_2, c_3, c_4\}$ can be estimated using linear least squares. The objective is then to find the wavenumber k which minimizes an error function, using a nonlinear optimization algorithm. The error function is computed between the real wave field $u^r(x_i, y_i, \omega)$ and the estimated wave field $u^e(x_i, y_i, \omega)$ such as:

$$\varepsilon = \sqrt{\frac{\sum_{i=1}^n |u^e(x_i, y_i, \omega) - u^r(x_i, y_i, \omega)|^2}{\sum_{i=1}^n |u^r(x_i, y_i, \omega)|^2}} \quad (10)$$

The damping loss factor η which is the structural damping of the material is identified by [48]:

$$\eta = \left| \frac{\Im\{k^4\}}{\Re\{k^4\}} \right| \quad (11)$$

The damping loss factor is related to the wave attenuation γ which is the spatial damping by: $\gamma = \eta/4$ [6].

2.3. Inhomogeneous Wave Correlation

The IWC method permits to explore the k-space content of a spatial field by correlation with inhomogeneous waves. The dispersion equations are fully reconstructed and the k-space characteristics are estimated. The standard form of the IWC method [5] allows accurate approximations in the mid-high frequency domain. Nevertheless, approximations are less accurate in the low frequency domain, particularly for damping, since the modal overlap is not sufficiently high to cover all propagation directions. To overcome this problem, some extended forms of the IWC method are proposed in literature [17, 18]. In this work, a special emphasis is put on the IWC variant (IWC-V) which has been proposed recently by Lajili et al. [13]. The IWC-V is based on an inhomogeneous wave correlation which accounts for both incident and reflected waves. However, only incident waves

are considered in the standard form of the IWC. The spatial field is correlated with a sum of inhomogeneous waves such as:

$$u_{IWCV} = e^{-ik(\theta)(1+i\gamma(\theta))(x \cos(\theta)+y \sin(\theta))} + e^{ik(\theta)(1+i\gamma(\theta))(x \cos(\theta)+y \sin(\theta))} \quad (12)$$

where the first term corresponds to incident or forward traveling waves and the second term to reflected or backward traveling waves.

The correlation between the spatial field and the inhomogeneous waves is ensured by a criterion which must be maximized. For a spatial field which is measured at n discrete locations, this criterion is expressed as:

$$IWCV(k, \gamma, \theta) = \frac{|\sum_n \rho_i \hat{u}(x_i, y_j) \cdot u_{IWCV}^*(x_i, y_j) S_i|}{\sqrt{\sum_n \rho_i |\hat{u}(x_i, y_j)|^2 S_i \cdot \sum_n \rho_i |u_{IWCV}(x_i, y_j)|^2 S_i}} \quad (13)$$

where u_{IWCV}^* is the complex conjugate of the wave u_{IWCV} . S_i is the elementary surface of the structure around a measurement point M_i and ρ_i is the coherence of measurement data at point M_i . This criterion represents the wave contribution in the field \hat{u} or also the ratio between the energy carried by the wave and the total energy contained in the field.

In practice [5, 22], the algorithm of application of the IWC-V method consists in putting the direction θ , for each frequency iteration, into a discrete set of values θ_j . For each direction θ_j , the maximal value of the $IWCV(k_j, \gamma_j, \theta_j)$ criterion corresponds to a couple of values (k_j, γ_j) of the wavenumber and the wave attenuation, respectively. The triplet $(k_j, \gamma_j, \theta_j)$ is removed if the $IWCV(k_j, \gamma_j, \theta_j)$ is too low, which means that the wave transports very low energy, or if the wave is strongly damped (for example $\gamma_j > 1$), which means that the wave does not transport energy (overdamped or evanescent).

2.4. Equivalent dynamic properties of 2D orthotropic structures

To provide equivalent dynamic properties of 2D orthotropic structures, the Love-Kirchhoff model is used. This model permits, in the case of elliptic orthotropy, to express the dispersion equation as:

$$k^4(\theta) \left(\sqrt{\tilde{D}_x} \cos^2(\theta - \theta_\perp) + \sqrt{\tilde{D}_y} \sin^2(\theta - \theta_\perp) \right)^2 = \omega^2 \quad (14)$$

where $\tilde{D} = D/\rho h$ and θ_\perp is an orthotropy angle between the reference axis and the orthotropy axis. The dynamic stiffnesses D_x , D_y and D_{xy} are defined in general orthotropy case by:

$$D_x = \frac{h^3}{12} \frac{E_x}{1-\nu_x \nu_y}, \quad D_y = \frac{h^3}{12} \frac{E_y}{1-\nu_x \nu_y}, \quad D_{xy} = \frac{h^3}{12} \left(\frac{\nu_y E_x}{1-\nu_x \nu_y} + \frac{\nu_x E_y}{1-\nu_x \nu_y} + 4G \right) \quad (15)$$

where E_x and E_y are the Young moduli in directions x and y , ν_x and ν_y are the Poisson' ratios, ρ the mass density and G the shear modulus:

$$G = \frac{1}{2} \frac{\sqrt{E_x E_y} - \nu_y E_x}{1 - \nu_x \nu_y} \quad (16)$$

The aim is then to define the parameters $\left\{ \theta_\perp, d_x = \sqrt{\tilde{D}_x}, d_y = \sqrt{\tilde{D}_y}, d_{xy} = 2\sqrt{\tilde{D}_x \tilde{D}_y} \right\}$.

Given $\vec{u}_{\theta_{\perp}}$ a symmetry axis of orthotropic behavior: $\forall \theta, k(\theta - \theta_{\perp}) = k(-\theta - \theta_{\perp})$ and $k(\theta) = k(-\theta - 2\theta_{\perp})$. To estimate the orthotropy angle θ_{\perp} , we need to maximize a cross-correlation function $\mathcal{R}(\Delta\theta)$:

$$\begin{aligned}\mathcal{R}(\Delta\theta) &= \frac{1}{2\pi} \int_0^{2\pi} k(\theta)k(-\theta - \Delta\theta) d\theta \\ &= \frac{1}{2\pi} \int_0^{2\pi} k(\theta)k(\theta + 2\theta_{\perp} - \Delta\theta) d\theta\end{aligned}\quad (17)$$

$\mathcal{R}(\Delta\theta)$ is maximum for $\Delta\theta = 2\theta_{\perp}$. In practice, referring to [21], if $\theta_{\perp} \in [0 \pi]$ the $\mathcal{R}(\Delta\theta)$ will be evaluated over $[0 2\pi]$ ($\Delta\theta_{\max} = 2\theta_{\perp}$), using $k \in [-2\pi 2\pi]$. The size of k_i and θ_i must then be doubled such as: $\forall i \in \mathbb{l}_{\theta}, \theta_{-i} = \theta_i - 2\pi$ and $k_{-i} = k_i$.

The dynamic flexural stiffnesses \tilde{D}_x and \tilde{D}_y of the equivalent orthotropic plate are estimated using linear least squares, using the error function:

$$\varepsilon(d_x, d_y) = \sum_{i \in \mathbb{l}_{\theta}} \left(d_x c_i + d_y s_i - \frac{\omega}{k_i^2} \right)^2 \quad (18)$$

where $c_i = \cos(\theta_i - \theta_{\perp})$ and $s_i = \sin(\theta_i - \theta_{\perp})$. This error function is minimum if $\overline{\text{grad}} \varepsilon(d_x, d_y) = 0$. Then d_x and d_y are computed by solving:

$$\begin{bmatrix} d_x \\ d_y \end{bmatrix} = \begin{bmatrix} \sum c_i^4 & \sum c_i^2 s_i^2 \\ \sum c_i^2 s_i^2 & \sum s_i^4 \end{bmatrix}^{-1} \begin{bmatrix} \sum c_i^2 \frac{\omega}{k_i^2} \\ \sum s_i^2 \frac{\omega}{k_i^2} \end{bmatrix} \quad (19)$$

Finally, orthotropy parameters $\{\theta_{\perp}, \tilde{D}_x = d_x^2, \tilde{D}_y = d_y^2\}$ are defined from $(\theta_i, k_i)_{i \in \mathbb{l}_{\theta}}$.

Modal density of an orthotropic plate

Based on works performed in [38, 39], the dispersion equation writes, in polar coordinates:

$$\kappa^4(1 - \alpha^2 \sin^2(2\theta)) = \rho h \omega^2 \quad (20)$$

with [40]:

$$\begin{cases} k_x D_x^{1/4} = \kappa \cos \theta \\ k_y D_y^{1/4} = \kappa \sin \theta \end{cases} \quad (21)$$

and $\alpha^2 = \frac{1}{2} \left(1 - \frac{D_{xy}}{2\sqrt{D_x D_y}} \right) = \frac{1}{2} (1 - \beta)$ function of the orthotropy parameter $\beta = \frac{D_{xy}}{2\sqrt{D_x D_y}}$.

The area below the constant $\kappa(\omega, \theta)$ curve in the wavenumber plane (k_x, k_y) is a measure of the number of modes $N(\omega)$ below the angular frequency ω [40]:

$$N(\omega) = \frac{S\omega}{2\pi^2} \sqrt{\frac{\rho h}{D_x}} \left(\frac{D_x}{D_y} \right)^{\frac{1}{4}} F(\alpha) \quad (22)$$

where $F(\alpha) = \int_0^{\pi/2} (1 - \alpha^2 \sin^2(2\theta))^{-1/2} d\theta$.

The asymptotic modal density n_{∞} is then obtained by derivation of $N(\omega)$:

$$n_\infty = \frac{S}{2\pi} \sqrt{\frac{\rho h}{D_x}} \left(\frac{D_x}{D_y} \right)^{\frac{1}{4}} F(\alpha) \quad (23)$$

Taking into account the correction ϵ depending on boundary conditions, the modal density writes:

$$n(f) = n_\infty \left(1 + \epsilon \frac{\tilde{L}}{\sqrt{4\pi S \bar{f}}} \right) \quad (24)$$

with $\bar{f} = f n_\infty$, $\epsilon = -1/2$ for the hinged case, $\epsilon = -1$ for the clamped case, $\epsilon = +1$ for the free case and $\tilde{L} = \sqrt{\frac{\pi}{2F(\alpha)}} (D_x D_y)^{\frac{1}{8}} \left(\frac{2L_x}{\bar{D}(0, \theta_\perp)^{1/4}} + \frac{2L_y}{\bar{D}(\pi/2, \theta_\perp)^{1/4}} \right)$ where $\bar{D}(\theta, \theta_\perp) = (\sqrt{D_x} \cos^2(\theta - \theta_\perp) + \sqrt{D_y} \sin^2(\theta - \theta_\perp))^2$.

2.5. Uncertainty propagation

In this work, uncertainty propagation is carried out using two methods: LHS and gPC. The sample-based LHS method [32] consists in generating a succession of N deterministic computations $\{X(\xi^{(n)}), n = 1, \dots, N\}$ to approximate the parameter X , according to a set of random variables $\{\xi^{(n)}\}_{n=1}^N$. These variables are selected by partitioning the variability space into regions of equal probability and picking up one sampling point in each region. This technique requires a computing time lower than that required by the MCS [30] but remains computationally unaffordable since its accuracy is proportional to the number N . To overcome the prohibitive cost of such sample-based methods without a significant loss of accuracy, the gPC method [33, 34] represents an interesting alternative. The gPC expansion combines multivariate polynomials and deterministic coefficients such as:

$$X = \sum_{j=0}^P \hat{x}_j \psi_j(\xi) = \hat{X}^T \Psi(\xi) \quad (25)$$

where $\{\hat{x}_j\}_{j=0}^P$ are the $P + 1$ unknown deterministic coefficients and $\{\psi_j(\xi)\}_{j=0}^P$ the $P + 1$ multivariate polynomials of d independent random variables $\{\xi^{(n)}\}_{n=1}^d$, such as:

$$P + 1 = \frac{(d+p)!}{d!p!} \quad (26)$$

To compute the $\{\hat{x}_j\}_{j=0}^P$ coefficients and then solve the gPC expansion (25), a nonintrusive regression technique is used in this work. It consists in minimizing the difference between the gPC approximate solution \hat{X} and the exact solution \bar{X} through the expression:

$$\hat{X} = (\Psi^T \Psi)^{-1} \Psi^T \bar{X} = \Psi^+ \bar{X} \quad (27)$$

where $\Psi = \{\psi_j(\xi^{(n)})\}_{n=1, \dots, M, j=0, \dots, P}$ is the data matrix and Ψ^+ is its Moore-Penrose pseudoinverse. Here,

$\Xi = \{\xi^{(n)}\}_{n=1}^M$ is a set of M random variables corresponding to M exact solutions $\{\bar{X}(\xi^{(n)}), n = 1, \dots, M\}$, with $M \geq P + 1$. The efficiency and the stability of the regression approximate lies on the well conditioning the matrix $(\Psi^T \Psi)$ which depends on the choice of the set Ξ of M random variables. The selection technique used here is that referred in [35, 36, 37, 41, 42].

3. Robust experiment-based identification of a honeycomb sandwich plate

3.1. Experiments and objectives

Let consider a sandwich composite plate of dimensions $1 \times 1 \text{ m}^2$, which is freely suspended under bending load. The core of the plate is in aluminum honeycomb (Nida Nomex) of thickness 13 mm . The skin of the plate is made of laminated carbon fiber epoxy (Hexcel reference 43199) and is of thickness 0.5 mm of each side, with a 50% resin fiber ratio. The plate is excited with a white noise by an electrodynamic shaker (Brüel & Kjaer, 4810) at the position $(x=0.3 \text{ m}, y=0.5 \text{ m})$, Figure 1. A force sensor (Brüel & Kjaer Type 8001) permits to collect the injected force. The vibration field of the plate is measured by a Polytec Scanning Vibrometer (PSV-400) at 1849 measuring points ($\Delta x=0.0231$, $\Delta y=0.0230 \text{ m}$). The field is sampled and acquired using a Fourier analyzer interfaced with a Hewlett Packard Paragon 35654A sampler.

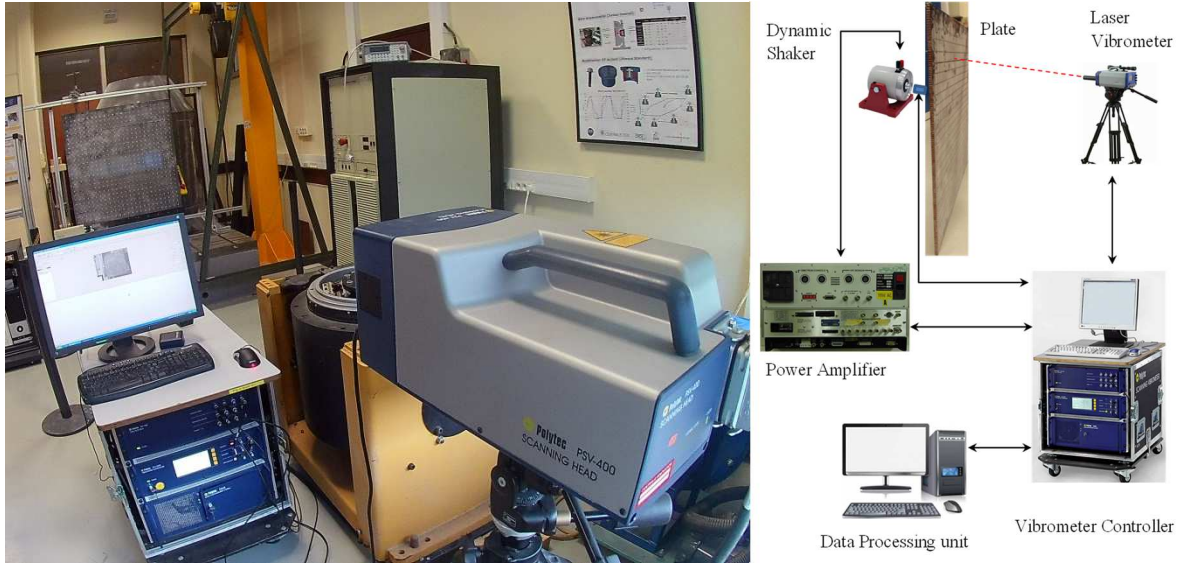


Fig.1. Experimental measuring configuration of the vibratory field of the sandwich plate with honeycomb core

The purpose of this study is to identify the k -space characteristics from the measured harmonic spatial field and then extract the equivalent mechanical parameters of the sandwich plate. A deterministic study is addressed at first to provide complete θ -dependent and frequency-dependent dispersion curves, damping (section 3.2) and equivalent orthotropic plate model (section 3.3). The identification is performed using the 2D-DFT, the Mc Daniel method, the IWC and the IWC-V which are compared to each other throughout the study. Then a stochastic study is carried out in section 3.4 taking into account a parametric uncertainty on the measurement points geometric coordinates. Such uncertainty quantifies the variability of the geometric coordinates when the measured vibratory field does not exactly match the associated measuring points due to experimental errors or manipulations. Stochastic identification processes which combine each identification method with either LHS or gPC method are applied. The impact of uncertainty on identifications is statically investigated and the robustness of the proposed identification processes against uncertainty is assessed.

3.2. k -space characteristics identification

The goal of this section is to provide complete θ -dependent and frequency-dependent dispersion curves and damping loss factor using the identification methods presented in section 2. The spatial 2D-DFT takes the advantage of a simple implementation and allows identifying the θ -dependent k -space profiles at discrete frequencies. These profiles correspond to the wavenumber variation in the 2D k -space which is also called wavenumber plane (k_x, k_y) . These profiles correspond to the maximums of

the real part of the transformation given by the 2D-DFT, Eqs. (1-2), which correspond to the transporting energy wavenumbers.

Figure 2 illustrates the k-space profiles identified by the 2D-DFT at some frequencies f_i arbitrarily chosen over the domain $[0, 3200 \text{ Hz}]$ ($f_i = \{542, 1066, 1960, 3200\} \text{ Hz}$). This figure shows also the measured velocity field at each frequency. In the mid-high frequency domain, the excitation point could be interpreted from the shapes of the velocity field, if it is not identified a priori. Figure 2 illustrates the geometry and frequency dependency of the k-space profiles. Moreover, elliptical shapes of the k-space profiles are illustrated and are more pronounced in the high frequency domain. The orthotropy of the sandwich plate is thus elliptic with an orthotropy angle approximately close to 0° . The orthotropy angle is computed in section 3.3. The discontinuity of the k-space profiles in the low frequency domain reveals the limits of the 2D-DFT which is typically a mid-high frequency method. In the low frequency domain, the energy is not evenly distributed in all propagation directions. Consequently, the wavenumber could not be identified in all directions. Furthermore, these results illustrate the increase of the wavenumber over the frequency domain due to the decrease of the wavelength which becomes large at low frequencies. The 2D-DFT results are compared with those obtained by the Mc Daniel method, which is considered as reference, Figure 3. Good agreement is obtained as shown at two arbitrarily chosen frequencies. The wavenumber is calculated using Eq. (4). Then the mean is computed at each frequency with respect to the propagation directions at which the maximums are defined. It should be noted that the discontinuity shown on the θ -dependent wavenumber variation is not deducible in the frequency-dependent variation illustrated in Figure 6(c). Indeed, the mean of the maximal values found for some propagation directions is computed at each frequency. Otherwise, values are filtered and only those transporting energy wavenumbers (maximums) are retained. Subsequently, smooth curves are obtained, even in the low-frequency domain, Figure 6(c). The 2D-DFT permits to identify the wave attenuation γ using the function $\Im\{\hat{u}\}/\Re\{\hat{u}\}$, based on the complex form of the wavenumber $k(1 + i\gamma)$. The wave attenuation is calculated using Eq. (5) with $\gamma_x \in [-\gamma_{max}, \gamma_{max}]$ and $\gamma_y \in [-\gamma_{max}, \gamma_{max}]$, Figure 5, $\gamma_{max} = 0.25$ being the theoretical maximal value of the wave attenuation. Eq. (6) permits to define the propagation direction θ for each maximum of $\Im\{\hat{u}\}/\Re\{\hat{u}\}$ and then the θ -dependent variation of the wave attenuation γ and the damping loss factor, $\eta = 4\gamma$. The identifications are performed at some (even few) propagation directions, Figure 4. Then, the mean with respect to the considered propagation directions leads to a smooth frequency-dependent curve, Figure 6(d). Subsequently, the 2D-DFT does not allow identifying a complete θ -dependent and frequency-dependent variation of the parameters.

Moreover, θ -dependent and frequency-dependent variations of the wavenumber and damping loss factor identified using the IWC-V are illustrated by 3D representations shown in Figure 6(a-b) respectively.

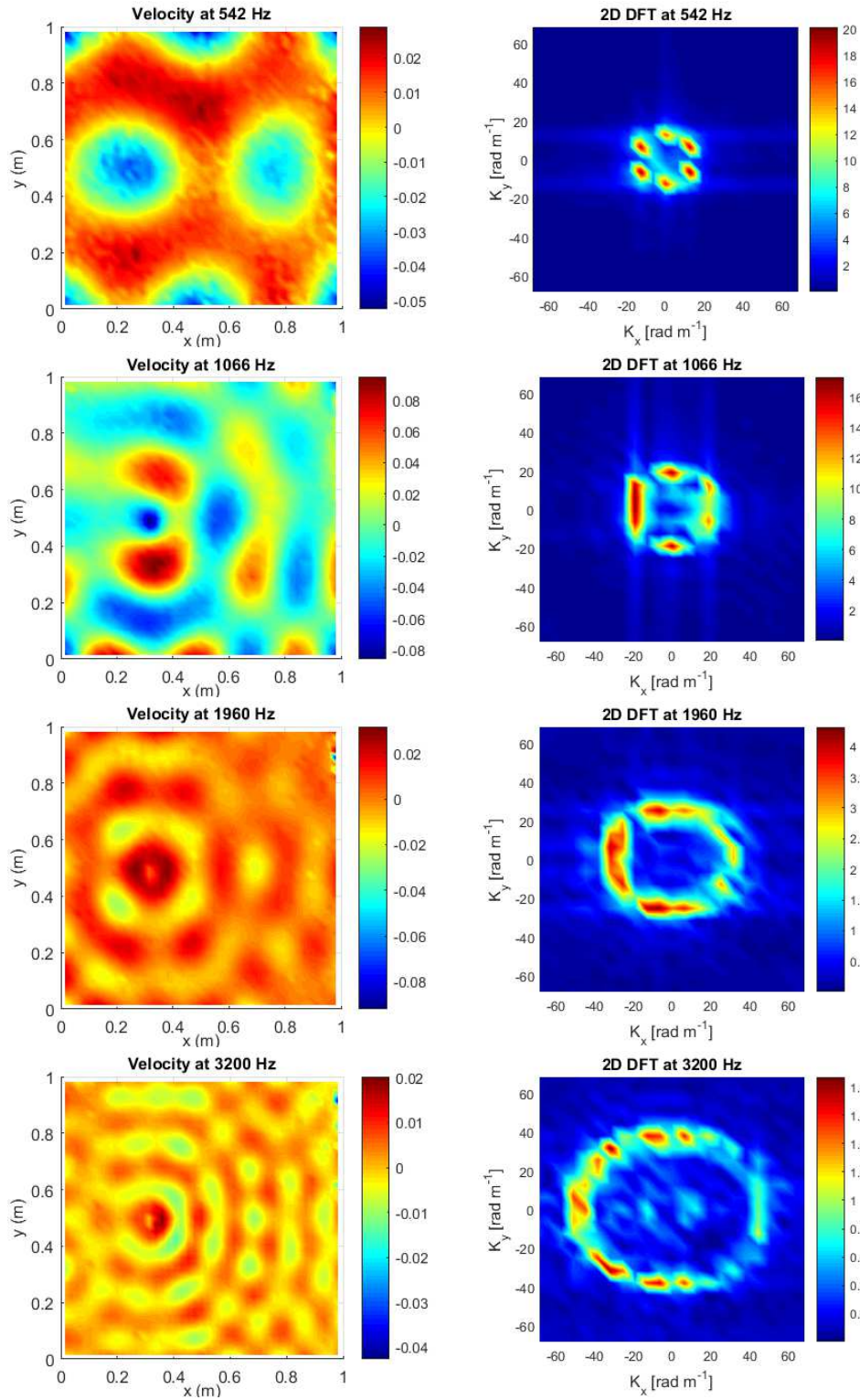


Fig.2. Velocity fields of the honeycomb sandwich plate and the associated k-space profiles identified by 2D-

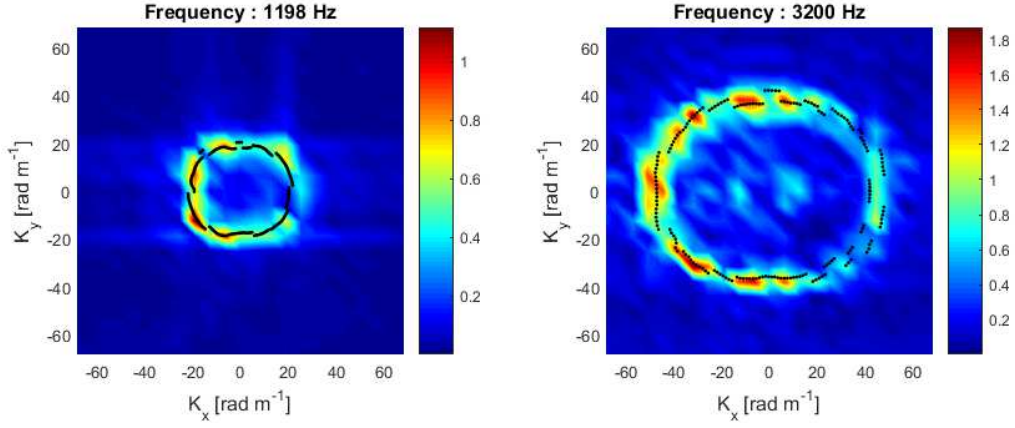


Fig.3. k-space profiles identified by the 2D-DFT method (colored surface plots) and the Mc Daniel method (black dotted curves) at two arbitrarily chosen frequencies

The identifications of the k-space characteristics using the Mc Daniel method, the IWC and the IWC-V are illustrated in Figures 4-6. Figure 4 shows polar representations of the θ -dependent variation of (a) the wavenumber, (b) the phase velocity c_φ ($k = \omega/c_\varphi$) and (c) the damping loss factor η , at some frequencies. The wavenumber and phase velocity profiles exhibit an elliptic orthotropic behavior of the honeycomb sandwich plate. Furthermore, the profiles vary from circular form to elliptic one which could be stretched in vertical or horizontal directions. This variation justifies the use of a frequency dependent orthotropic model to extract equivalent mechanical properties from wavenumber identifications, section 2.4. The elliptic shape of the k -profiles is pronounced proportionally to frequency. The inverse relation between the wavenumber and the phase velocity explains the inverted elliptical form of the c_φ -profiles (with an angle approximately close to 90°) compared to the k -profiles (orthotropy angle near to 0°). Moreover, the θ -dependence of these k-space characteristics is slightly smooth: no significant variation between consecutive directions.

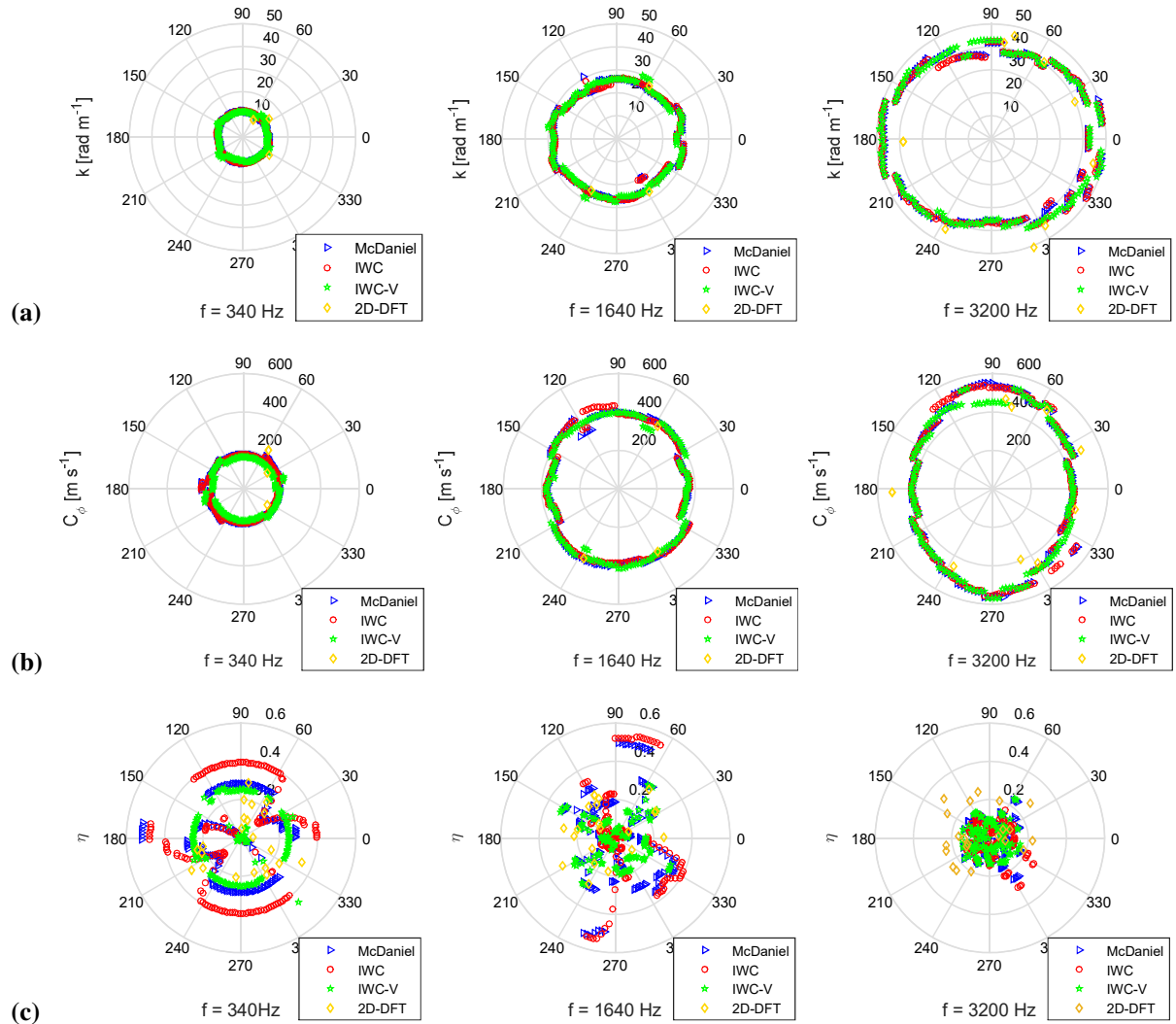


Fig.4. Polar θ -dependent variation of (a) the wavenumber, (b) the phase velocity and (c) the damping loss factor identified by Mc Daniel, IWC, IWC-V and 2D-DFT at frequencies 340 Hz, 1640 Hz and 3200 Hz

Nevertheless, the investigations of the damping loss factor identification reveal to be more complicated. Few works in the literature focus on such analysis, especially for 2D composite structures [6, 27]. Figure 4(c) illustrates strong θ -dependent variability of the damping loss factor and disagreement between all applied identification methods. The smoothness of the curves obtained at low frequencies does not reveal accurate identifications but wrong values. For the sake of brevity, only three polar representations are shown. The dispersed damping profiles make it difficult to compare the applied identification methods, despite the agreement which has been deduced in terms of amplitude. Frequency-dependent variation of the identified damping loss factor, Figure 6(d), shows oscillating values in the low-frequency domain.

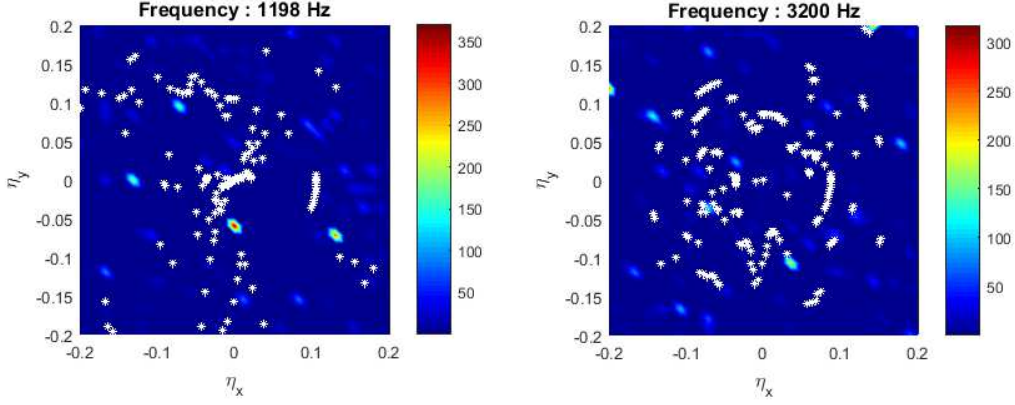


Fig.5. Cartesian representation of the damping loss factor profiles identified by the 2D-DFT method (colored surface plots) and the Mc Daniel method (white dotted curves) at two arbitrarily chosen frequencies

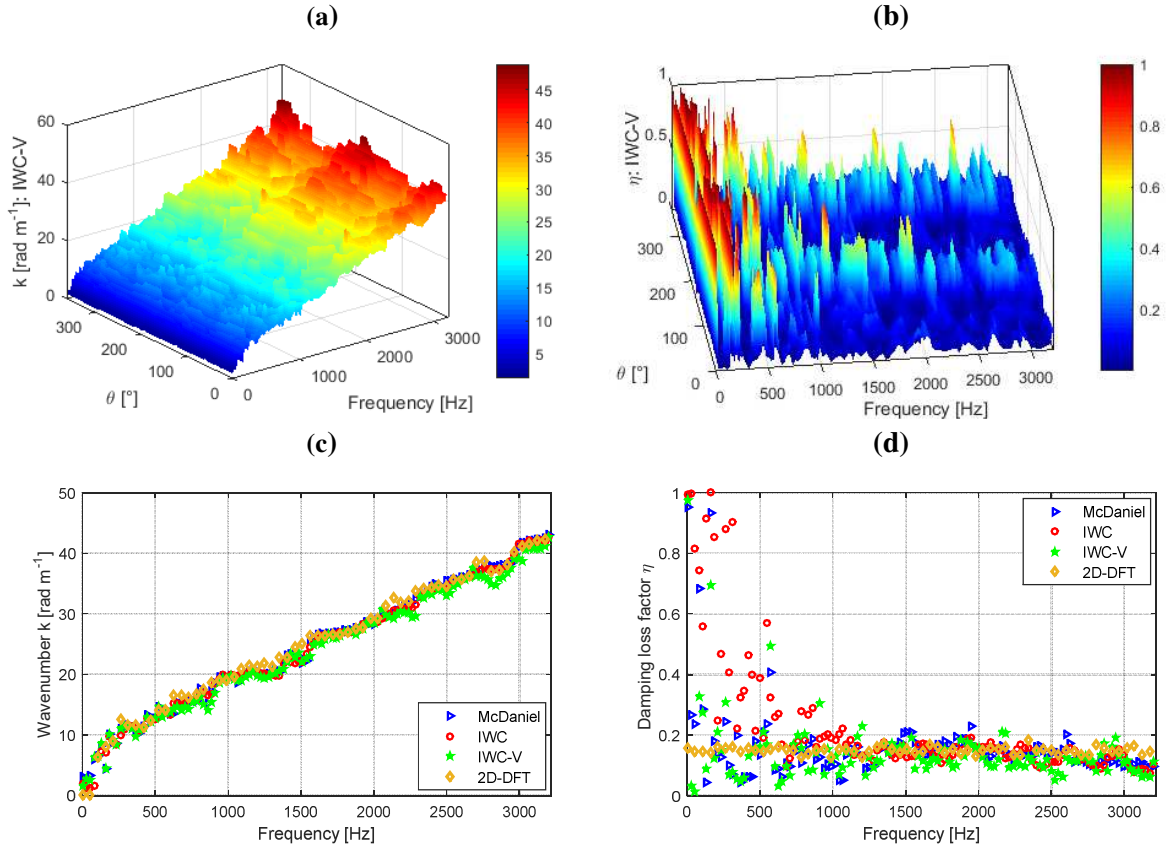


Fig.6. 3D representations of the frequency-dependent and propagation direction-dependent variation of (a) the wavenumber and (b) the damping loss factor identified using the IWC-V; Frequency-dependent variation of the mean values, computed with respect to all propagation directions, of (c) the wavenumber and (d) the damping loss factor identified using the Mc Daniel method, the IWC, the IWC-V and the 2D-DFT

Polar and cartesian representations of the k -space characteristics identification reveal an elliptic orthotropic behavior which permits to simplify investigations taking advantage of the symmetry. Nevertheless, the damping θ -dependent variation does not reveal any symmetrical profiles. Therefore, it is necessary to find out another criterion which could extract correlations between the identified values at different propagation directions. The Modal Assurance Criterion (MAC) is a comparison criterion which is in the literature to evaluate eigenvectors' correlation [37, 43]. In our case, a similar criterion is used to compute correlation indices between identified values at all propagation directions, for both wavenumber and damping loss factor. A matrix C is defined such as $C_{ij}(k) =$

$\|k_i^t \cdot k_j\| / (\|k_i\| \cdot \|k_j\|)$, where $k_i = k(\theta_i)$. $C_{ij} = 1$ indicates perfect correlation and thus perfect symmetry between directions θ_i and θ_j . $C_{ij} = 0$ means that no-correlation is found. Figure 7 illustrates the matrices $C(k)$ and $C(\eta)$ computed for the wavenumber and the loss factor, respectively. The $C_{ij}(k)$ values vary between 0.984 and 1 which illustrates multiple symmetries for the wavenumber. Much less symmetries are obtained for the loss factor since $C_{ij}(\eta) \in [0,1]$ with a tendency toward 0.

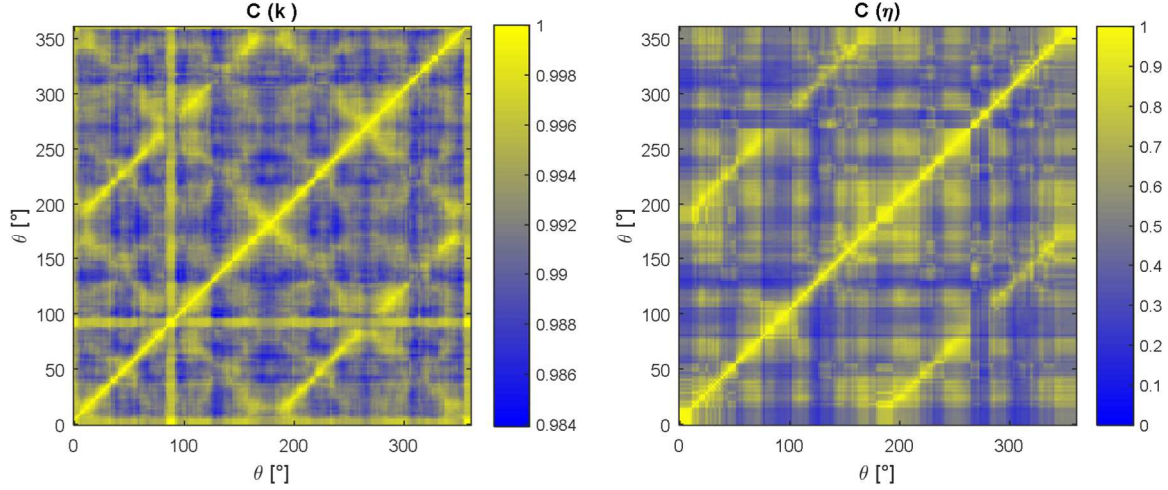


Fig.7. Correlation matrices $C(k)$ and $C(\eta)$ computed for the wavenumber and the loss factor, respectively

3.3. Equivalent dynamic properties extraction

The main purpose of this section is to extract relevant dynamic properties from the k-space characteristics, identified in section 3.2, using the model given in section 2.4. The orthotropy angle θ_{\perp} is computed using Eq. (17) with the hypothesis of no frequency-dependency. The θ_{\perp} is estimated by 3.5° using the three methods Mc Daniel, IWC and IWC-V, Figure 13, with very small relative errors. $\theta_{\perp} = 3.5^{\circ}$ in the majority of frequencies, excepting dispersed values at some frequencies as shown in Figure 8.

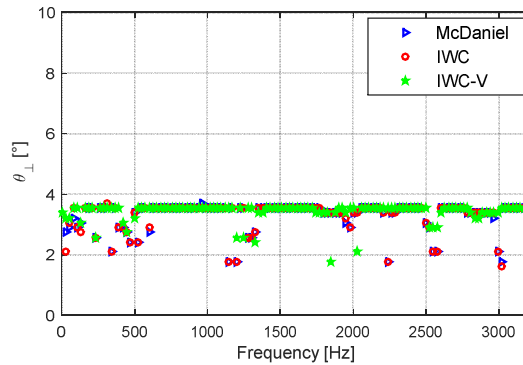


Fig.8. Orthotropy angle computed over the considered frequency domain using the Mc Daniel method, the IWC and the IWC-V

θ_{\perp} being calculated, the dynamic stiffnesses $\tilde{D}_x(f)$, $\tilde{D}_y(f)$ and $\tilde{D}_{xy}(f)$ and the mechanical parameters E_x , E_y , G , ν_x and ν_y are deduced. The frequency-dependent variation of these parameters is illustrated in Figure 9. Strong oscillations of the curves are detected at low frequencies and are progressively attenuated as the frequency increases. Non-monotonic variability is obtained, particularly at low frequencies. The k-space based methods are more efficient in the mid-high frequency domain. At low frequencies, the modal overlap is very low and few wavenumbers are

correctly defined which affects the dynamic stiffnesses identification. Note that the θ -dependent variation of the dynamic stiffnesses could also be investigated [44]. It should also be noted that several works in the literature focus on the identification of mechanical parameters of 1D and 2D structures. In [45, 46], composite beams characterizations were performed using an inverse method based on local equation of motion. Equivalent viscoelastic parameters were identified considering composite material as homogeneous. In [18, 47], equivalent models of heterogeneous composite and orthotropic sandwich plates were proposed to estimate the equivalent mechanical parameters.

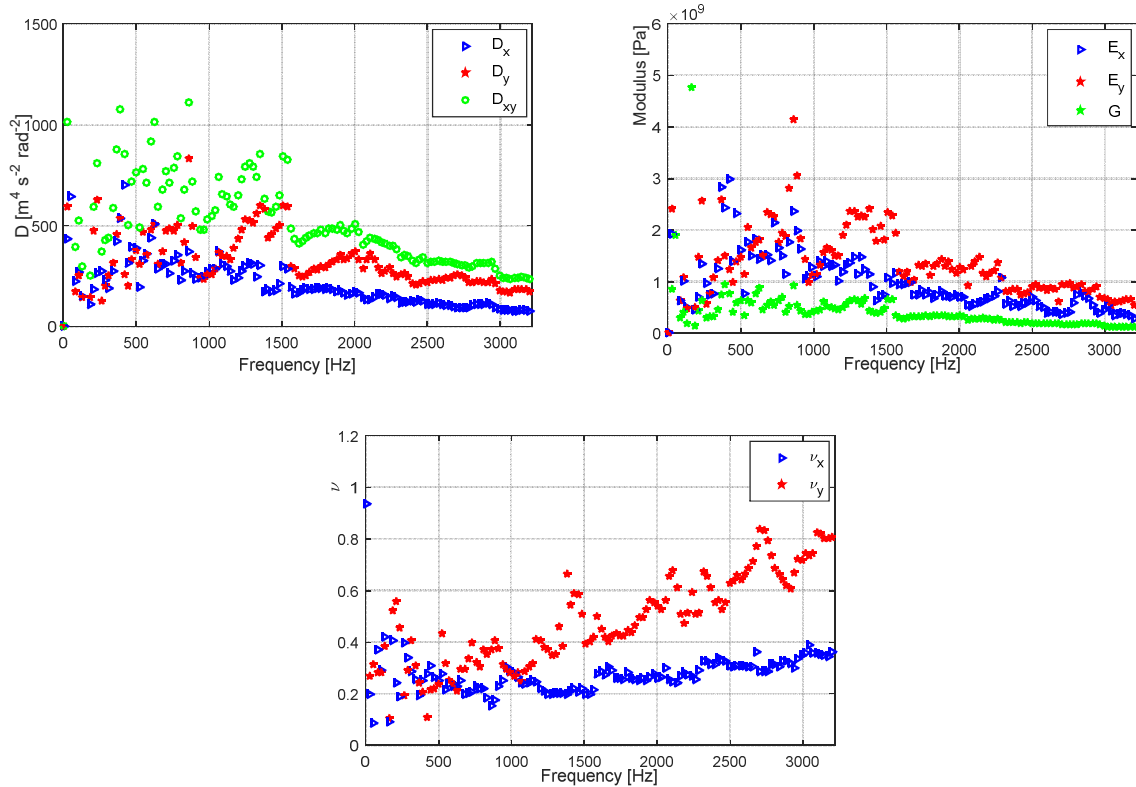


Fig.9. Frequency-dependent variation of the dynamic stiffness, the elasticity moduli and the Poisson's ratios identified using the IWC-V

Besides, the identified k-space characteristics and dynamic stiffnesses permit to estimate the modal density. The modal density is of fundamental importance in vibration mechanics. It represents an essential indicator in the mid-high frequency domain, with particular importance in the prediction of high-frequency vibration levels. In the literature, it is considered as a key parameter in several analyses approach to vibration prediction in a wide range of structural applications such as the statistical energy analysis method which allows investigating the influence of boundary conditions and mechanical properties. With special emphasis on the mid-high frequency domain, such indicator should be properly identified in the present work. The modal density is defined as the number of resonant modes within a unit frequency band. For the considered freely suspended sandwich plate with honeycomb core, the modal density increases as frequency increases, Figure 10. The modal density is computed using the formulation given by Renji et al. [38] and Boutillon et al. [39], section 2.4, based on the wavenumber identified using the Mc Daniel method, the IWC or the IWC-V. The curve becomes smoother and the individual resonances coalesce as the frequency increases. These results are coherent with those obtained by Renji et al. [38] and Clarkson and Ranky [49] for orthotropic honeycomb sandwich panels with shear.

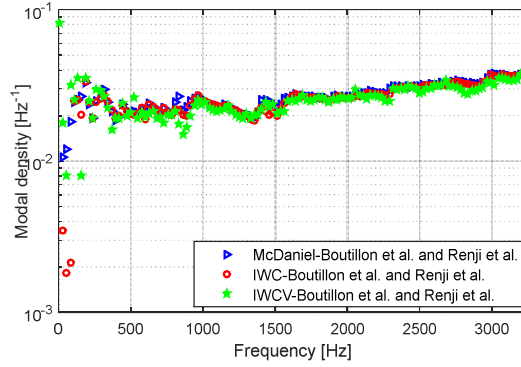


Fig.10. Frequency-dependent variation of the modal density of the sandwich plate with honeycomb core

3.4. Statistical investigations of the impact of uncertainty on the k-space characteristics identification

Deterministic hypothesis in experiment-based structural identification remains constraining in vibration mechanics. The analysis should be sensitive even to the smallest perturbation or ignorance which could occur during experiments. Realistic investigations require therefore accounting for such perturbation which could essentially be random. The most influencing parametric variability should be linked to the measurement of the vibratory field which is the main input of the identification process. For instance, the measured vibratory field may not match the associated measuring points' coordinates. In a probabilistic framework, these coordinates could vary randomly in the (x, y) plane such as $X = X_0(1 + \delta_X \xi)$, where X is the measurement points' coordinates matrix, X_0 the vector containing mean values, δ_X the statistical dispersion value and ξ a gaussian random variable. The uncertainty on the input parameters is propagated through the identification model in order to investigate its impact on the output results. 1000 samples-based LHS method is used to propagate uncertainty. It allows for accurate results, which could be considered as reference, but is very time consuming. Alternatively, the gPC method allows for an interesting computational time reduction without a significant loss of accuracy [36, 37]. Several stochastic identification processes are constructed by combining each identification method with either LHS or gPC methods and are compared to each other. These processes are denoted hereafter: LHS-2D-DFT, LHS-McDaniel, LHS-IWC, LHS-IWC-V and gPC-IWC-V. Statistical investigations of the robustness analysis against uncertainty are carried out. Statistical post-processing quantities are computed: the mean, the envelope (extreme statistics) and the statistical dispersion which is the ratio of the standard deviation by the mean. The impact of uncertainty on the identified wavenumber is illustrated in Figure 11 which compares the results of the processes LHS-2D-DFT and LHS-McDaniel, in a cartesian representation (a), and those of the processes LHS-McDaniel, LHS-IWC and LHS-IWC-V, in polar representations (b), at frequency 3200 Hz.

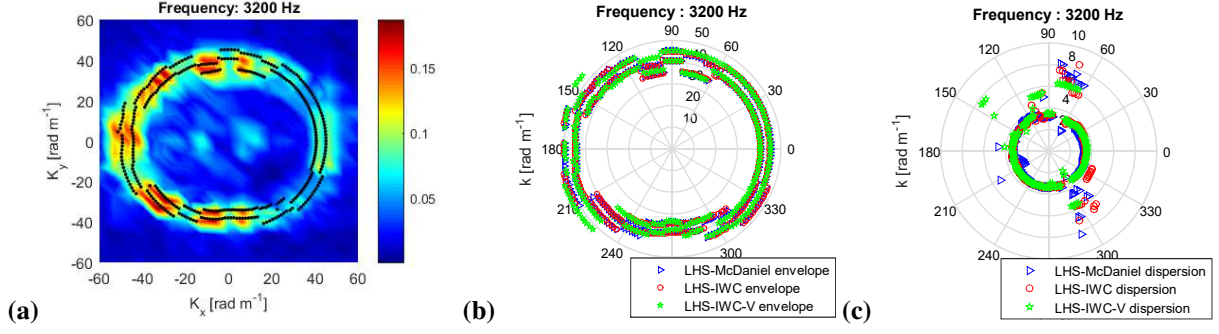


Fig.11. (a) Cartesian representation of the envelopes of the k-space profiles estimated using the LHS-McDaniel and the LHS-2D-DFT processes at frequency 3200 Hz; Polar representations of (b) the envelopes and (c) the statistical dispersions of the k-space profiles identified using the LHS-McDaniel, the LHS-IWC and the LHS-IWC-V processes at frequency 3200 Hz

Figure 12 illustrates the variation of the envelope and the statistical dispersion of the wavenumber over the considered frequency domain. The width of the envelope increases as the frequency increases and a nearly constant statistical dispersion of around 3.5% is obtained. These results show that a statistical dispersion of 2% of the measurement points' coordinates affects significantly the wavenumber identification. The LHS-IWC-V identification process allows more accurate identifications compared to the gPC-IWC-V process. The LHS-IWC-V process proves to be robust against uncertainty with a very interesting gain on computational time which reaches 99.51%.

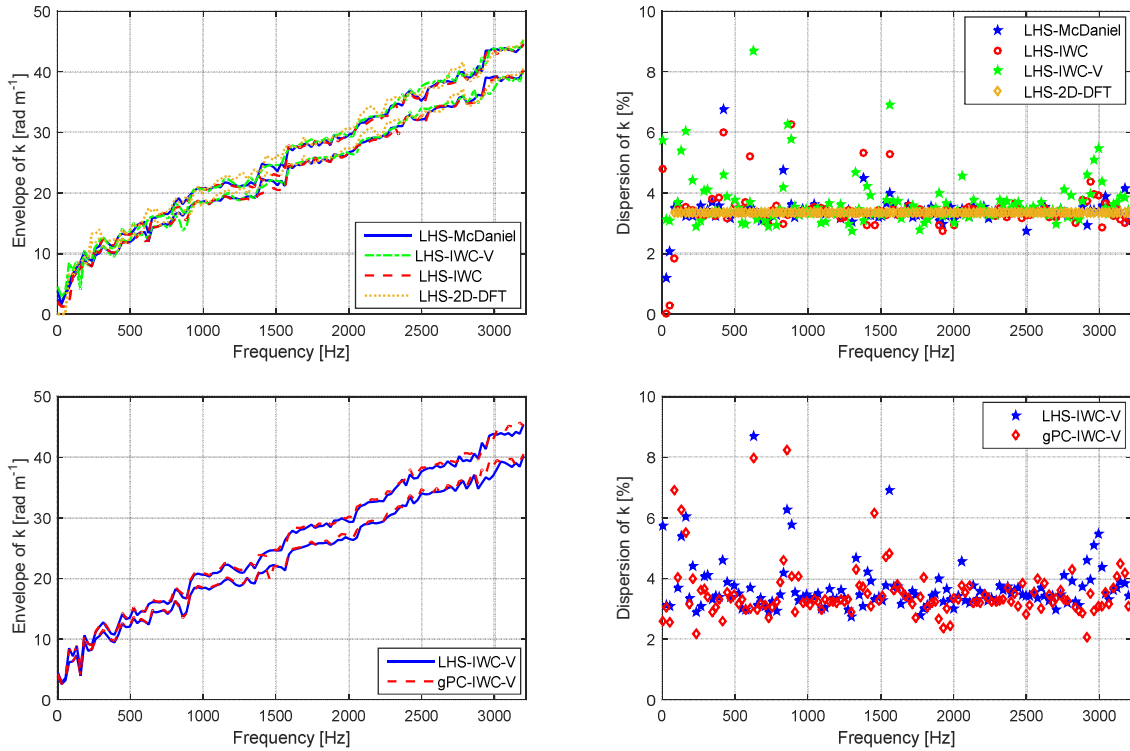


Fig.12. Envelopes and statistical dispersions of the wavenumber computed over the considered frequency domain using the identification processes LHS-2D-DFT, LHS-McDaniel, LHS-IWC, LHS-IWC-V and gPC-IWC-V

Generally smooth elliptic profiles describe the wavenumber variation in the k-space. Similar shapes are found for the phase velocity, but results are not shown for the sake of brevity. Nevertheless, disordered polar distributions are obtained for the damping. The analysis is more complicated and few works focus on this issue in the literature. The variations over the considered frequency domain of the

envelope and the statistical dispersion of the wave attenuation are illustrated in Figure 11. A nearly constant envelope and a statistical dispersion of 3.5% are obtained. Results are compared to those published by the authors in their previous work [13] which has addressed numerical-based and experiment-based identification of isotropic and sandwich beams. It has been illustrated that uncertainty on the measurement points' coordinates does not affect the damping loss factor estimate. A statistical dispersion equal to zero has been found for the damping loss factor.

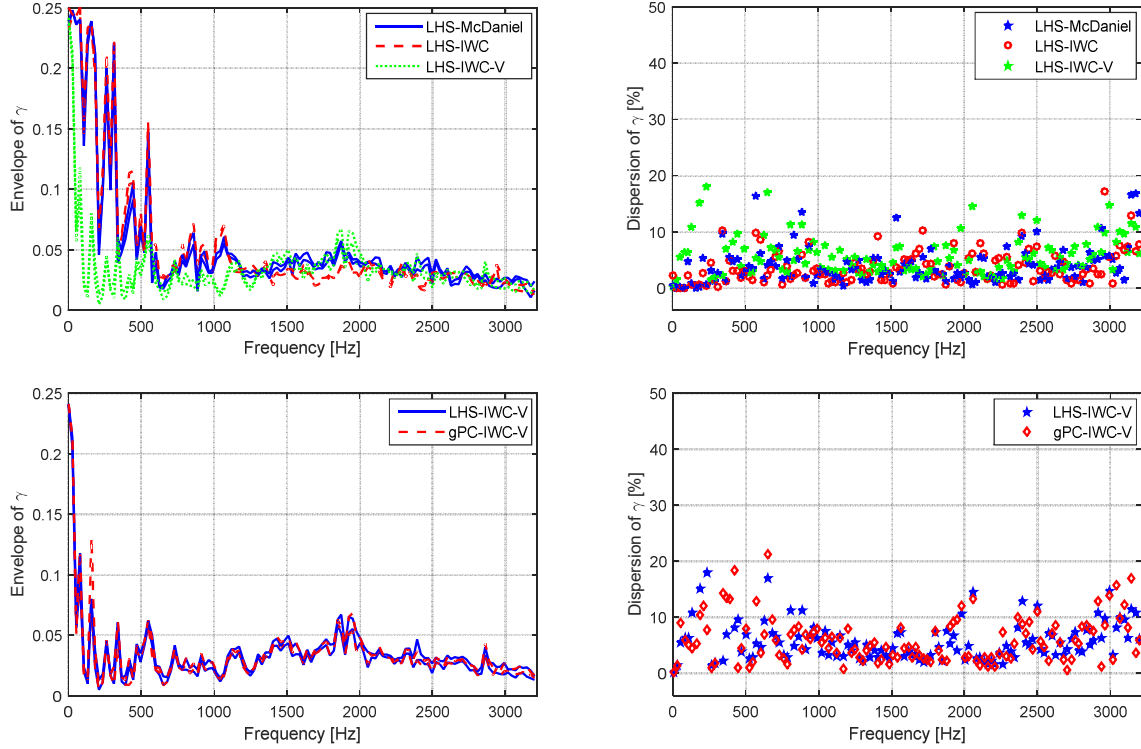


Fig.13. Envelopes and statistical dispersions of the wave attenuation computed over the considered frequency domain using the identification processes LHS-McDaniel, LHS-IWC, LHS-IWC-V and gPC-IWC-V

Furthermore, an illustration of the impact of uncertainty on the damping loss factor is provided by the correlation matrix C , Figure 14. The C_{ij} correlation indices are here computed between deterministic values of the loss factor and the means of the stochastic ones. Compared to the matrix C computed in deterministic case, Figure 7, which is recalled in Figure 14(a), the correlation is no longer perfect on the diagonal terms, Figure 14(b). Indeed, the impact of uncertainty is illustrated mainly by diagonal terms which are no longer equal to one: $C_{ij} < 1$, Figure 14(b).

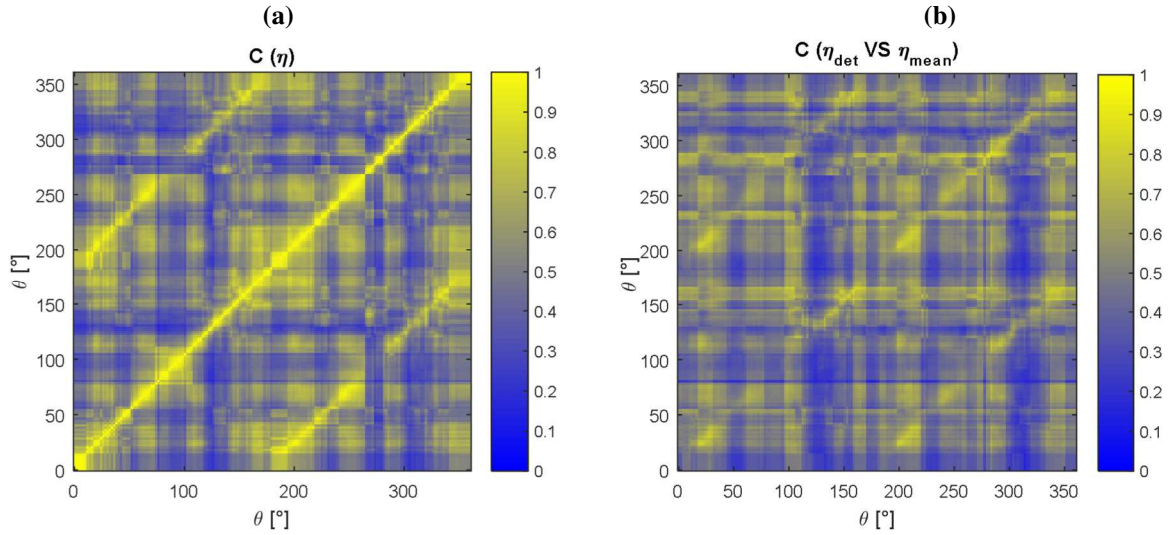


Fig.14. Comparison of the correlation matrices \mathcal{C} computed for the damping loss factor in (a) deterministic case and (b) stochastic case: (a) the correlation indices are computed at each propagation direction between the value of the loss factor and the values at all other propagation directions; (b) the correlation indices are computed at each propagation direction between the deterministic value of the loss factor and the mean values of the stochastic loss factor at all other propagation directions.

To recapitulate, the statistical investigations show that the impact of the uncertainty of the measurement points' coordinates on the k-space characteristics' estimates is significant, which reveals the sensitivity of identification to erroneous experimental manipulations leading to such uncertainty. The analysis highlights besides the robustness of the processes combining identification and uncertainty propagation methods.

3.5. Statistical investigations of the impact of uncertainty on the equivalent dynamic properties

The purpose of this section is to investigate the impact of uncertainty on the orthotropy angle, the dynamic stiffnesses, the modal density and the mechanical parameters which are computed using the identified stochastic k-space characteristics. Figure 15 shows the statistical quantifications (mean and envelope) of the orthotropy angle variability over the considered frequency domain in the stochastic case. A statistical dispersion of nearly 20% is obtained, against only 2%-dispersed measurement points' coordinates. The identification of the orthotropy characteristics is thus strongly affected by such uncertain measurement data.

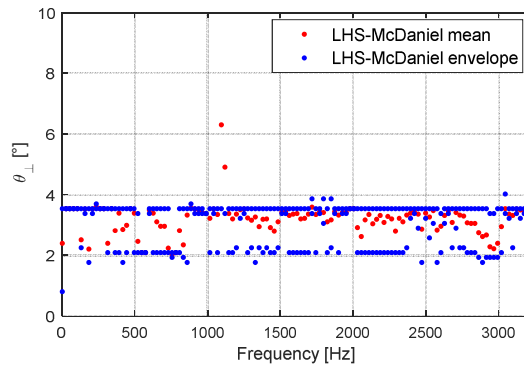


Fig.15. Mean and envelope of the orthotropy angle computed over the considered frequency domain using the identification process LHS-McDaniel

Figures 16-19 illustrate the statistical quantifications of the variability of the dynamic stiffnesses and the mechanical parameters over the considered frequency domain. Only results corresponding to \tilde{D}_x , $n(f)$, E_x and ν_x are shown for the sake of brevity. Statistical dispersions of nearly 13.5%, 13.5%, 15%, 17% and 7% are obtained on the dynamic stiffnesses \tilde{D}_x , \tilde{D}_y and \tilde{D}_{xy} , the modal density $n(f)$, the Young Moduli E_x and E_y , the shear Modulus G and the Poisson's ratios ν_x and ν_y , respectively, Tab. 1. These statistical dispersion values reflect the important impact of the measurement points' coordinates variability on the identification of the mechanical parameters of the honeycomb sandwich plate.

Tab.1. Statistical dispersions of the identified parameters

Parameter	Input		Outputs												
	X	k	c_φ	γ	η	θ_\perp	\tilde{D}_x	\tilde{D}_y	\tilde{D}_{xy}	$n(f)$	E_x	E_y	G	ν_x	ν_y
Dispersion (%)	2	3.5		3.5		20	13.5			13.5	15		17	7	

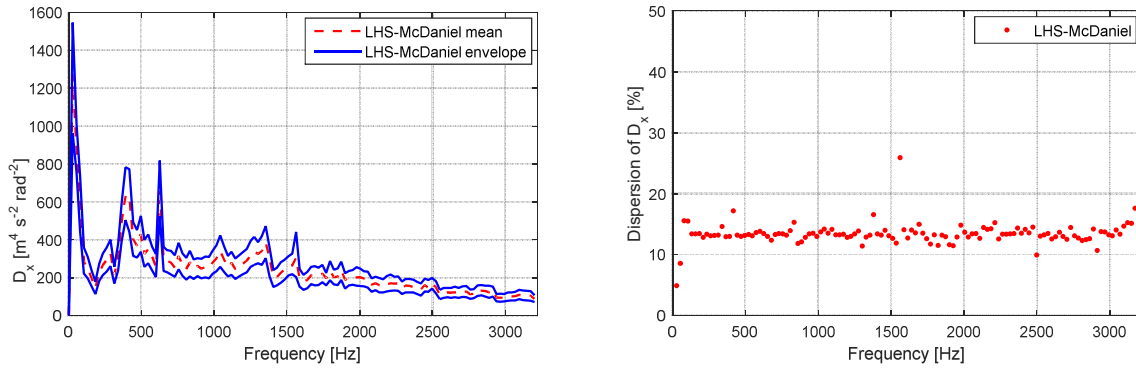


Fig.16. Envelope and statistical dispersion of the dynamic stiffness \tilde{D}_x computed over the considered frequency domain using the identification process LHS-McDaniel

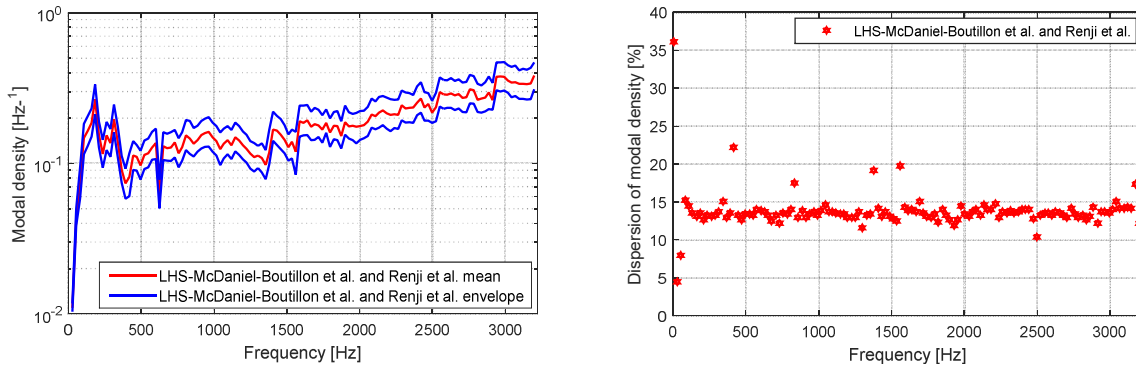


Fig.17. Envelope and statistical dispersion of the modal density computed over the considered frequency domain using the identification process LHS-McDaniel

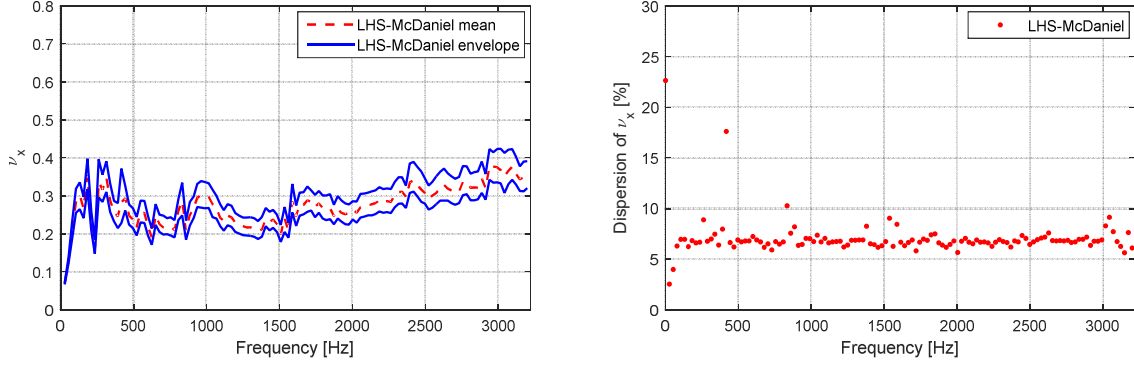


Fig.18. Envelope and statistical dispersion of the Poisson's ratio ν_x computed over the considered frequency domain using the identification process LHS-McDaniel

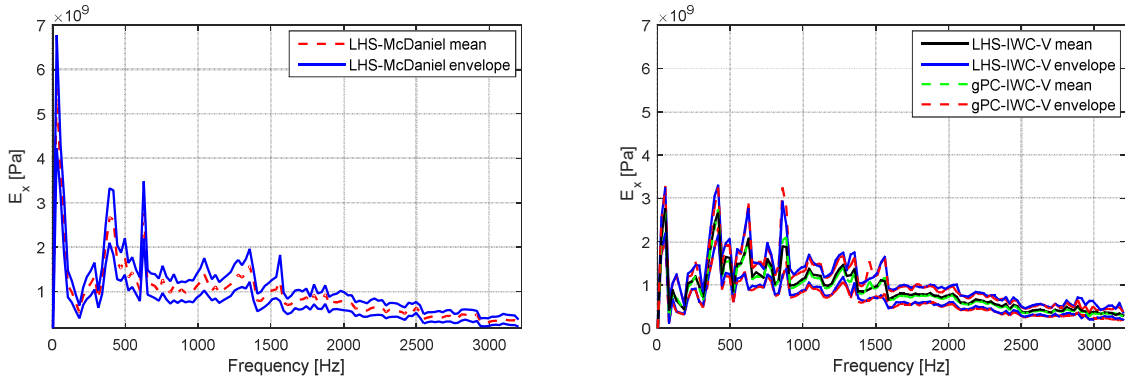


Fig.19. Envelope and statistical dispersion of the Young Modulus E_x computed over the considered frequency domain using the identification processes LHS-McDaniel, LHS-IWC-V and gPC-IWC-V

Otherwise, a statistical dispersion of 2% on the measurement points' coordinates is multiplied by nearly 1.7 when identifying the wavenumber, the phase velocity, the wave attenuation and the damping loss factor. It is then four-times greater when calculating the orthotropy angle, the dynamic stiffnesses, the modal density, the elastic and shear moduli and the Poisson's ratios.

Concerning the proposed identification processes, good agreement is obtained between the results of the LHS-IWC-V process and those of the gPC-IWC-V process. We highlight the advantages of the gPC method regarding the LHS method in terms of computational time, without a significant loss of accuracy.

4. Conclusion

The present paper has investigated the impact of the random variability of the measurement points' coordinates on the identification of both spatial and structural characteristics of a sandwich plate with honeycomb core over a large frequency domain. The identification process is based on measured velocity field and carried out to estimate the spatial characteristics in the wave propagation space and then extract the structural parameters using an equivalent elliptic orthotropic model. Several stochastic two-dimensional experiment-based identification processes have been proposed and compared to each other. A special emphasis is put on the process combining the Variant of the Inhomogeneous Wave Correlation method and the generalized Polynomial Chaos method. The process has proven to be robust against the significant variability estimated on the identified parameters with a very important computational time reduction and without a significant loss of accuracy. Statistical investigations of the uncertainty impact have illustrated an important output-to-input statistical dispersion ratio which

reveals the identification sensitivity to such measuring errors involved in experimental manipulations. The intensity of the uncertainty impact differs from one parameter to another and increases as the identification procedure progresses, reaching a four-times greater statistical dispersion for the shear modulus.

Uncertainty on the measurement points' coordinates is not the only influencing factor which could affect the identification process. It should be interesting to consider other types of uncertainties, either parametric or nonparametric. Sensitivity analyses could also be addressed to determine on which parameters the identification might be dependent and sensitive, which optimizes the needs of the engineer throughout the execution of the identification process.

References

1. K. Grosh, E.G. Williams, Complex wave-number decomposition of structural vibrations, *J. Acoust. Soc. Amer.* 93 (1993) 836-848. <https://doi.org/10.1121/1.405445>.
2. N.S. Ferguson, C.R. Halkyard, B.G. Mace, K.H. Heron, The estimation of wavenumbers in two dimensional structures, *Proc. ISMA*, 2002, pp. 799-806.
3. J. G. McDaniel, P. Dupont, L. Savino, A wave approach to estimating frequency-dependent damping under transient loading, *J. Sound Vib.* 231 (2000) 433-449. <https://doi.org/10.1006/jsvi.1999.2723>.
4. J. Berthaut, M.N. Ichchou, L. Jezequel, Identification in large frequency range of effective parameters of two-dimensional structures by means of wave numbers, *Mecanique & Industries*. 4 (2003) 377-384. [https://doi.org/10.1016/S1296-2139\(03\)00073-3](https://doi.org/10.1016/S1296-2139(03)00073-3).
5. J. Berthaut, M.N. Ichchou, L. Jezequel, K-space identification of apparent structural behavior, *J. Sound Vib.* 280 (2005) 1125-113. <https://doi.org/10.1016/j.jsv.2004.02.044>.
6. F. Marchetti, K. Ege, Q. Leclère, N.B. Roozen, On the structural dynamics of laminated composite plates and sandwich structures; a new perspective on damping identification, *J. Sound Vib.* 474 (2020) 115256. <https://doi.org/10.1016/j.jsv.2020.115256>.
7. N.B. Roozen, Q. Leclère, K. Ege, Y. Gerges, Estimation of plate material properties by means of a complex wavenumber fit using Hankel's functions and the image source method, *J. Sound Vib.* 390 (2017) 257-271. <https://doi.org/10.1016/j.jsv.2016.11.037>.
8. J. Cuenca, F. Gautier, L. Simon, The image source method for calculating the vibrations of simply supported convex polygonal plates, *J. Sound Vib.* 322 (4) (2009) 1048–1069. <https://doi.org/10.1016/j.jsv.2008.11.018>.
9. F. Marchetti, N.B. Roozen, J. Segers, K. Ege, M. Kersemans, Q. Leclère, Experimental methodology to assess the dynamic equivalent stiffness properties of elliptical orthotropic plates, *J. Sound Vib.* 495 (2021) 115897. <https://doi.org/10.1016/j.jsv.2020.115897>.
10. P. Margerit, A. Lebé, J.-F. Caron, X. Boutillon, High Resolution Wavenumber Analysis (HRWA) for the mechanical characterisation of viscoelastic beams, *J. Sound Vib.* 433 (2018) 198-211, <https://doi.org/10.1016/j.jsv.2018.06.062>
11. P. Margerit, A. Lebé, J.-F. Caron, K. Ege, X. Boutillon, The High-Resolution Wavevector Analysis for the characterization of the dynamic response of composite plates, *J. Sound Vib.* 458 (2019) 177–196, <https://doi.org/10.1016/j.jsv.2019.06.026>
12. G. Tufano, F. Errico, O. Robin, C. Droz, M.N. Ichchou, B. Pluymers, W. Desmet, N. Atalla, K-space analysis of complex large-scale meta-structures using the Inhomogeneous Wave Correlation method, *Mech. Syst. Sign. Process.* 135 (2020) 106407. <https://doi.org/10.1016/j.ymsp.2019.106407>.

13. R. Lajili, O. Bareille, M.-L. Bouazizi, M.N. Ichchou, N. Bouhaddi, Composite beam identification using a variant of the inhomogeneous wave correlation method in presence of uncertainties, *Eng. Computation*. 35 (2018) 2126-2164. <https://doi.org/10.1108/EC-03-2017-0072>.
14. J. Berthaut, Contribution à l'identification Large Bande Des Structures Anisotropes: Application Aux Tables d'harmonie Des Pianos Ph.D. thesis, École Centrale de Lyon, France, 2004.
15. G. Inquiété, Numerical simulation of wave propagation in laminated composite plates Ph.D. thesis, Ecole Centrale de Lyon, France, 2008.
16. R. Cherif, J.-D. Chazot, N. Atalla, Damping loss factor estimation of two-dimensional orthotropic structures from a displacement field measurement, *J. Sound Vib.* 356 (2015) 61-71. <https://doi.org/10.1016/j.jsv.2015.06.042>.
17. L. Van Belle, C. Claeys, E. Deckers, W. Desmet, On the impact of damping on the dispersion curves of a locally resonant metamaterial: Modeling and experimental validation, *J. Sound Vib.* 409 (2017) 1-23. <https://doi.org/10.1016/j.jsv.2017.07.045>.
18. N.B. Roozen, L. Labelle, Q. Leclère, K. Ege, S. Alvarado, Non-contact experimental assessment of apparent dynamic stiffness of constrained-layer damping sandwich plates in a broad frequency range using a Nd:YAG pump laser and a laser Doppler vibrometer, *J. Sound Vib.* 395 (2017) 90-101. <https://doi.org/10.1016/j.jsv.2017.02.012>.
19. D. Alleyne, Cawley P. (1991), A two-dimensional Fourier transform method for the measurement of propagating multimode signals, *J. Acoust. Soc. Am.* 89 (1991) 1159-1168. <https://doi.org/10.1121/1.400530>.
20. J.S. Bolton, H.J. Song, Y.K. Kim, Y.J. Kang, The Wave Number Decomposition Approach to the Analysis of Tire Vibration, *Proc. Noise*, 1998, pp. 97-102.
21. M.N. Ichchou, O. Bareille, J. Berthaut, Identification of effective sandwich structural properties via an inverse wave approach, *Eng. Struct.* 30 (2008) 2591-2604. <https://doi.org/10.1016/j.engstruct.2008.02.009>.
22. M.N. Ichchou, J. Berthaut, M. Collet, Multi-mode wave propagation in ribbed plates: Part I, wavenumber-space characteristics, *Int. J. Solids Struct.* 45 (2008) 1179-1195. <https://doi.org/10.1016/j.ijsolstr.2007.09.032>.
23. T. Huang, Multi-modal propagation through finite elements applied for the control of smart structures Ph.D. thesis, Ecole Centrale de Lyon, France, 2012.
24. M. Ruzek, J.-L. Guyader, C. Pézerat, Information criteria and selection of vibration models, *J. Acoust. Soc. Am.* 136 (2014) 3040-3050. <https://doi.org/10.1121/1.4900562>.
25. C.W. Zhou, Wave and modal approach for multi-scale analysis of periodic structures Ph.D. thesis, Ecole Centrale de Lyon, France, 2014.
26. C.W. Zhou, J.P. Lainé, M.N. Ichchou, A.M. Zine, Numerical and experimental investigation on broadband wave Propagation features in perforated plates, *Mech. Syst. Sign. Process.* 75 (2016) 556-575. <https://doi.org/10.1016/j.ymsp.2015.12.006>.
27. N.B. Roozen., L. Labelle, Q. Leclère, K. Ege, Y. Gerges, Estimation of plate material properties by means of a complex wavenumber fit using Hankel's functions and the image source method, *J. Sound Vib.* 390 (2017) 257-271. <https://doi.org/10.1016/j.jsv.2016.11.037>.
28. B. Van Damme, A. Zemp, Measuring Dispersion Curves for Bending Waves in Beams: A Comparison of Spatial Fourier Transform and Inhomogeneous Wave Correlation, *Acta Acust united Ac.* 104 (2018) 228-234. <https://doi.org/10.3813/AAA.919164>.
29. G.S. Fishman, Monte Carlo: Concepts, Algorithms, and Applications. Springer-Verlag, 1996. <https://doi.org/10.1007/978-1-4757-2553-7>.

30. R.Y. Rubinstein, D.P. Kroese, *Simulation and the Monte Carlo Method*, second ed. A John Wiley & Sons, New York, 2008. <https://doi.org/10.1002/9780470230381>.
31. M.D. McKay, R.J. Beckman, W.J. Conover, A comparison of three methods for selecting values of input variables in the analysis of output from a computer code, *Technometrics*. 21 (1979) 239-245. <https://doi.org/10.2307/1268522>.
32. J.C. Helton, F.J. Davis, Latin hypercube sampling and the propagation of uncertainty in analyses of complex systems, *Reliab. Eng. Syst. Saf.* 81 (2003) 23-69. [https://doi.org/10.1016/S0951-8320\(03\)00058-9](https://doi.org/10.1016/S0951-8320(03)00058-9).
33. D. Xiu, G.E. Karniadakis, The Wiener-Askey polynomial chaos for stochastic differential equations, *SIAM J. Sci. Comput.* 24 (2002) 619-644. <https://doi.org/10.1137/S1064827501387826>.
34. C. Soize, R. Ghanem, Physical systems with random uncertainties: Chaos representation with arbitrary probability measure, *SIAM J. Sci. Comput.* 26 (2004) 395-410. <https://doi.org/10.1137/S1064827503424505>.
35. M. Berveiller, B. Sudret, M. Lemaire, Stochastic finite elements: a non intrusive approach by regression, *Eur. J. Comput. Mech.* 15 (2006) 81-92. <https://doi.org/10.3166/remn.15.81-92>.
36. K. Chikhaoui, D. Bitar, N. Kacem, N. Bouhaddi, Robustness Analysis of the Collective Nonlinear Dynamics of a Periodic Coupled Pendulums Chain, *Appl. Sci.*, 7 (2017) 684. <https://doi.org/10.3390/app7070684>.
37. K. Chikhaoui, N. Bouhaddi, N. Kacem, M. Guedri, M. Soula, Uncertainty quantification/propagation in nonlinear models: robust reduction - generalized polynomial chaos, *Eng. Computation*. 34 (2017) 1082-1106. <https://doi.org/10.1108/EC-11-2015-0363>.
38. K. Renji, P.S. Naira, S. Narayanan, Modal density of composite honeycomb sandwich panels, *J. Sound Vib.* 195 (1996) 687-699. <https://doi.org/10.1006/jsvi.1996.0456>.
39. X. Boutillon, K. Ege, Vibroacoustics of the piano soundboard: Reduced models, mobility synthesis, and acoustical radiation regime, *J. Sound Vib.* 332 (2013) 4261-4279. <https://doi.org/10.1016/j.jsv.2013.03.015>.
40. J.P.D. Wilkinson, Modal Densities of Certain Shallow Structural Elements, *J. Acoust. Soc. Am.* 43 (1968) 245-251. <https://doi.org/10.1121/1.1910773>.
41. B. Sudret, Global sensitivity analysis using polynomial chaos expansions, *Reliab. Eng. Syst. Saf.* 93 (2008) 964-979. <https://doi.org/10.1016/j.ress.2007.04.002>.
42. G. Blatman, B. Sudret, An adaptive algorithm to build up sparse polynomial chaos expansions for stochastic finite element analysis, *Probabilistic Eng. Mech.* 25 (2010) 183-197. <https://doi.org/10.1016/j.probenmech.2009.10.003>.
43. D.J. Ewins, *Modal Testing : Theory, Practice and Application*. Wiley, 2000.
44. F. Ablitzer, C. Pézerat, B. Lascoup, J. Brocaïl, Identification of the flexural stiffness parameters of an orthotropic plate from the local dynamic equilibrium without a priori knowledge of the principal directions, *J. Sound Vib.* 404 (2017) 31-46. <https://doi.org/10.1016/j.jsv.2017.05.037>.
45. T. Wassereau, *Caractérisation de matériaux composites par problème inverse vibratoire* Ph.D. thesis, Université du Maine, France, 2016.
46. T. Wassereau, F. Ablitzer, C. Pézerat, J.-L. Guyader, Experimental identification of flexural and shear complex moduli by inverting the Timoshenko beam problem, *J. Sound Vib.* 399 (2017) 86-103. <https://doi.org/10.1016/j.jsv.2017.03.017>.
47. F. Ablitzer, C. Pézerat, J.-M. Génevaux, J. Bégué, Identification of stiffness and damping properties of plates by using the local equation of motion, *J. Sound Vib.* 333 (2014) 2454-2468. <https://doi.org/10.1016/j.jsv.2013.12.013>.

48. M. Rak, M. Ichchou, J. Holnicki-Szul, Identification of structural loss factor from spatially distributed measurements on beams with viscoelastic layer, *J. Sound Vib.* 310 (2008) 801-811. <https://doi.org/10.1016/j.jsv.2007.11.026>.
49. Clarkson, M. F. Ranky, Modal density of honeycomb plates, *J. Sound Vib.* 91(1) (1983), 103-118. [https://doi.org/10.1016/0022-460X\(83\)90454-6](https://doi.org/10.1016/0022-460X(83)90454-6).
- 50.